ACS OMEGA

http://pubs.acs.org/journal/acsodf

Article

# A pH and $Mg^{2+}$-Responsive Molecular Switch Based on a Stable DNA Minidumbbell Bearing 5′ and 3′-Overhangs

Jiacheng Zhang,[#] Yang Wang,[#] Liqi Wan, Yuan Liu,[*] Jie Yi, Sik Lok Lam, and Pei Guo[*]

Cite This: *ACS Omega* 2021, 6, 28263−28269

Read Online

ACCESS | Metrics & More | Article Recommendations | Supporting Information

**ABSTRACT:** Minidumbbell (MDB) is a non-B DNA structure of which the thermodynamic stability is sensitive to a chemical environment such as pH, serving as a potential structural motif in constructing DNA-based molecular switches. This work aims to design thermodynamically stable MDB structures bearing 5′ and 3′-overhanging deoxyribonucleotides in order to examine the possibility of MDB to be functionalized. Via making use of 5-methylcytosine and adjusting the pH of solution to be acidic, MDBs bearing 1-nucleotide (nt) or 2-nt overhanging residues at the 5′ and 3′-ends have been obtained. Based on one of the new MDB sequences, we have designed a molecular switch that could respond to dual inputs of pH and $Mg^{2+}$. The MDB strand and its partner strand formed a duplex (the "ON" state) upon inputting pH 7 and $Mg^{2+}$, whereas the duplex dissociated to restore the MDB structure (the "OFF" state) upon inputting pH 5 and EDTA. The demonstration on the ability of MDB to sustain 5′ and 3′-overhanging residues and the construction of a pH and $Mg^{2+}$-responsive molecular switch will extend the application of MDB structures in dynamic DNA nanotechnology.

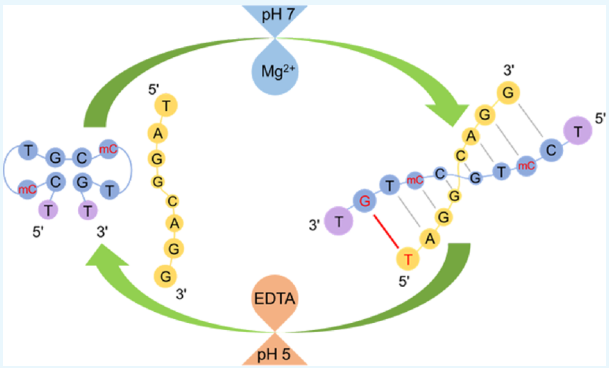


## 1. INTRODUCTION

A DNA molecule can exist in various conformations apart from the classical B-form structure. Non-B DNAs, such as the triplex,[1] G-quadruplex,[2] and i-motif,[3] have been found to associate with different biological functions and genetic instabilities.[4] In recent years, non-B DNAs have attracted extensive attentions owing to their potential applications in DNA nanotechnology. In particular, molecular switches based on non-B DNAs can respond to a variety of inputs such as pH, metal ions, and light,[5−7] offering an advantage over those governed solely by Watson−Crick base pairs.[6] The non-B DNA, which is sensitive to chemical change, can serve as a template to guide the assembly of metal nanoparticles[8,9] and control drug release[10,11] and can also be used as a probe in biosensing when reporter molecules are conjugated with the non-B DNA.[12,13] These properties, supplemented with their biocompatibility, pose the non-B DNA as a promising structural candidate in bio-related research.

Minidumbbell (MDB) is a non-B DNA structure formed by eight to ten-nucleotide sequences.[14,15] It is composed of two tetraloops or pentaloops with extensive interactions between intraloop and interloop residues. For the MDBs containing two type II tetraloops, the first (L1/L1′) and fourth (L4/L4′) loop residues form a loop-closing base pair, the second loop residue (L2/L2′) sits in the minor groove, and the third loop residue (L3/L3′) stacks on the nearby loop-closing base pair in each loop (Figure 1).[14] The MDB structures have been found to form in expandable CCTG and ATTCT repeats of which

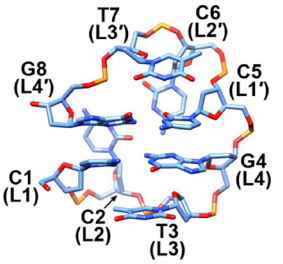


**Figure 1.** Averaged NMR solution structure of the MDB containing two CCTG tetraloops (PDB ID: 5GWL).

expansion mutations associate with myotonic dystrophy type 2 and spinocerebellar ataxia type 10 neurodegenerative diseases, respectively, suggesting a potential role of MDB in mediating genetic instabilities of these repeats.[14,15] It has been proposed that MDBs could escape from mismatch repair via a competing mechanism.[16] Small ligands that can target the MDBs may offer a strategy for disease therapy.[4] Apart from its potential biological roles, the MDB has been utilized to construct

**Received:** August 12, 2021
**Accepted:** September 21, 2021
**Published:** October 14, 2021





https://doi.org/10.1021/acsomega.1c04346
*ACS Omega* 2021, 6, 28263−28269

chemical stimuli-responsive molecular switches.[17,18] For instance, upon repeatedly adjusting the pH from 7 to 5 and vice versa, formation and dissociation of a DNA duplex could be controlled in a reversible manner at room temperature.[17] Due to the small molecular size, MDB-based molecular switches were easier to be manipulated compared to those using triplexes[19] and quadruplexes[6] formed by longer sequences or those relying on strand displacement.[20]

Further functionalization of MDB, such as conjugation with gold nanoparticle, lipophilic moiety, and fluorophore/quencher, will greatly extend the application of MDB. However, the ability of MDB to sustain functional modification depends on whether the thermodynamic stability of MDB is high enough, as any chemical addition at the termini of an MDB is expected to weaken the 5′ and 3′-terminal stacking that is essential to the MDB formation. So far, all reported MDBs formed by natural sequences have mild thermodynamic stabilities, *i.e.,* their melting temperature ($T_m$) values ranged from 17 to 46 °C,[14,15,17,21,22] and it is unclear whether MDBs are stable enough to be functionalized. This work aims to investigate if any MDBs can sustain functional modifications. We added 5′ and 3′-overhanging residues at the termini of the MDB to mimic the presence of functional modifications. Their structures and thermodynamic stability were examined using solution nuclear magnetic resonance (NMR) and ultraviolet (UV) spectroscopy, respectively. It was found that MDBs formed by natural sequences could not sustain overhanging residues. Upon using 5-methylcytosine (mC) and adjusting the pH of solution to be acidic, stable MDBs bearing 5′ and 3′-overhanging residues were obtained. On the basis of a newly designed sequence, we have constructed a DNA molecular switch that could switch to the "ON" state (a duplex) upon inputting pH 7 and $Mg^{2+}$ and switch back to the "OFF" state (two separated strands) upon inputting pH 5 and EDTA. Results of this work pave the way for functionalization of MDBs and extend their applications in dynamic DNA nanotechnology.

## 2. RESULTS AND DISCUSSION

All DNA sequences used in this study are shown in Table 1. We first investigated if the MDB formed by 5′-CCTGCCTG-3′ at pH 5 could sustain 5′ and 3′-overhangs, as this sequence formed the most stable MDB among all reported natural sequences,[17] and it was named as $(CCTG)_2$ here. Based on this model sequence, we designed two sequences by adding (i) a 5′-T and a 3′-T and (ii) a 5′-A and a 3′-T to $(CCTG)_2$, which were named as $T(CCTG)_2T$ and $A(CCTG)_2T$, respectively. Further, we modified the core MDB-forming sequence in $T(CCTG)_2T$ and $A(CCTG)_2T$ by substituting its minor groove cytosine residues (C2 and C6) with 5-methylcytosine residues (mC2 and mC6). The two newly obtained sequences were named as $T(CmCTG)_2T$ and $A(CmCTG)_2T$, respectively. To investigate if the methylated MDBs could sustain extra overhanging residues, a sequence named as $TT(CmCTG)_2TT$ was designed. For constructing a DNA molecular switch based on $T(CmCTG)_2T$, two sequences were used, including 5′-CAGGCAGG-3′ and 5′-TAGGCAGG-3′, which were named as *S1-wc* and *S2-tg*, respectively.

**Table 1. DNA Sequences Used in this Study**

| name | sequence |
|---|---|
| $(CCTG)_2$ | 5′-CCTGCCTG-3′ |
| $T(CCTG)_2T$ | 5′-TCCTGCCTGT-3′ |
| $A(CCTG)_2T$ | 5′-ACCTGCCTGT-3′ |
| $T(CmCTG)_2T$ | 5′-TCmCTGCmCTGT-3′ |
| $A(CmCTG)_2T$ | 5′-ACmCTGCmCTGT-3′ |
| $TT(CmCTG)_2TT$ | 5′-TTCmCTGCmCTGTT-3′ |
| *S1-wc* | 5′-CAGGCAGG-3′ |
| *S2-tg* | 5′-TAGGCAGG-3′ |

**2.1. MDB Was Unable to Form in $T(CCTG)_2T$ and $A(CCTG)_2T$.** We first study the solution structures of $T(CCTG)_2T$ and $A(CCTG)_2T$ to examine if the MDB could sustain 5′ and 3′-overhanging residues, which were a mimic of adding functional modifications at the two termini of MDBs. In the reported $(CCTG)_2$ MDB at pH 5,[17] (i) C1 and C2 were fully protonated at their N3 sites, (ii) $C1^+$-G4 and C5-G8 formed the Hoogsteen and Watson−Crick loop-closing base pairs, respectively, (iii) $C2^+$ and C6 formed a reverse wobble mispair via three hydrogen bonds, and (iv) T3 and T7 stacked on $C1^+$-G4 and C5-G8 base pairs, respectively (Figure 2A). These structural features lead to corresponding NMR features, including (i) the downfield shifted $C1^+$ and $C2^+$ amino H41/H42 proton signals at ∼9.0 to 10.5 ppm due to protonation at their N3 sites, (ii) the $C1^+$ H3 signal at ∼17.0 ppm in the $C1^+$-G4 Hoogsteen base pair and the G8 H1 signal at ∼13.0 ppm in the C5-G8 Watson−Crick base pair, (iii) C6 H41/H42 at ∼8.5/6.9 ppm together with $C2^+$ H41/H42 at ∼9.8/9.3 ppm in the $C2^+$·C6 reverse wobble mispair, and (iv) upfield shifted T3 and T7 H7 signals at ∼1.4 ppm due to the shielding effect of their nearby loop-closing base pairs.[17] Based on the reference NMR spectrum of the $(CCTG)_2$ MDB, we first acquired 1D $^1$H NMR spectra for $T(CCTG)_2T$ and $A(CCTG)_2T$.

Figure 2B,C shows the 1D $^1$H NMR spectra of $T(CCTG)_2T$ and $A(CCTG)_2T$ at pH 7, 6, and 5 in comparison with the reference spectrum of $(CCTG)_2$ MDB at pH 5. Unfortunately, upon lowering the pH from 7 to 5, we did not observe any characteristic NMR signals belonging to the MDB in $T(CCTG)_2T$ and $A(CCTG)_2T$, such as the $C1^+$ H3 signal at ∼17 ppm, G8 H1 signal at ∼13 ppm, $C1^+$ and $C2^+$ H41/H42 signals at 9.0−10.5 ppm, and upfield shifted T3 and T7 H7 signals at ∼1.4 ppm, revealing that the MDB was not formed in these two sequences.

The original $(CCTG)_2$ MDB has a $T_m$ value of ∼46 °C, yet an addition of 5′ and 3′-overhanging residues lead to the failure in forming an MDB even at 0 °C. The result suggested that 5′ and 3′-overhanging residues strongly destabilized the MDB structure. This is different from the effects of overhanging residues on DNA duplexes or G-quadruplexes, wherein addition of one or two overhanging residues could stabilize the structures via gaining base−base stackings between the overhanging residues and terminal base pairs[23] and G-tetrads.[24,25] However, in the case of MDB structures, the overhanging residues might weaken the base−base stacking between the 3′-terminal G8 and 5′-terminal $C1^+$, which is crucial to the MDB formation. Therefore, designing thermodynamically more stable MDBs that can compensate the destabilization caused by overhanging residues appears to be the prerequisite for functionalization of MDBs.

**2.2. $T(CmCTG)_2T$ and $A(CmCTG)_2T$ Formed Stable MDB Structures.** Previously, we have reported that hydrophobic interactions between the methyl groups of minor groove residues and the 2′-methylene groups of loop-closing base pair residues provided substantial stabilization to the


https://doi.org/10.1021/acsomega.1c04346
ACS Omega 2021, 6, 28263−28269

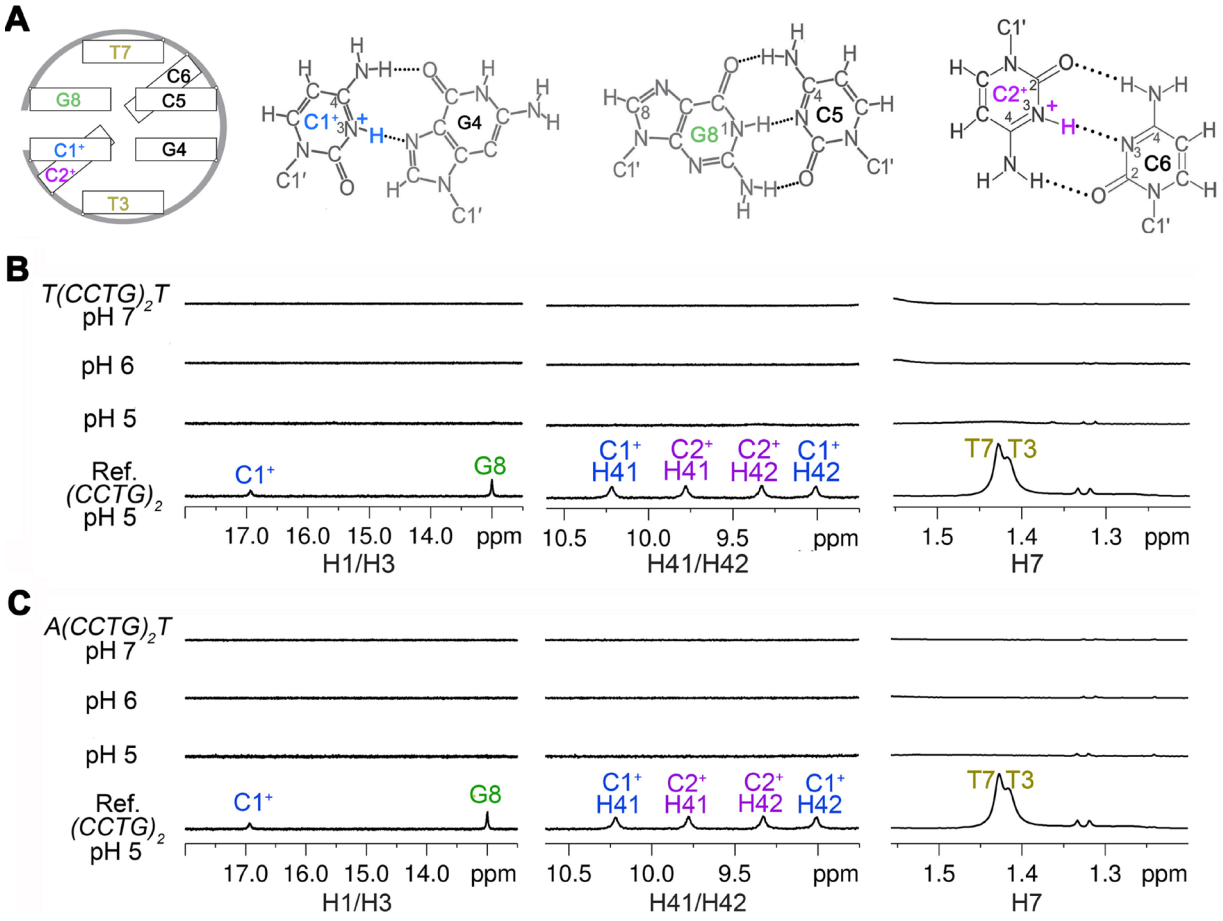


**Figure 2.** (A) Schematic of the $(CCTG)_2$ MDB. (B, C) 1D $^1$H NMR spectra of $T(CCTG)_2T$ and $A(CCTG)_2T$ at pH 7, 6, and 5 in comparison with the reference spectrum of $(CCTG)_2$ MDB at pH 5. All spectra were acquired at 0 °C. The H1/H3 and H41/H42 signal intensities were amplified by fourfolds relative to the methyl H7 signals.

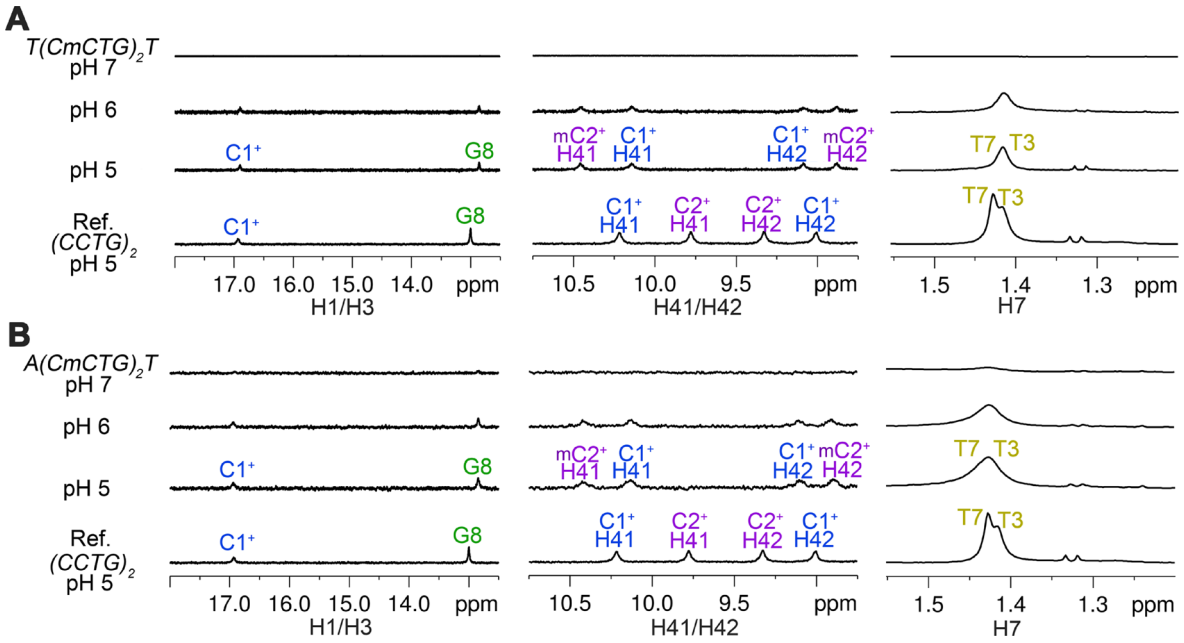


**Figure 3.** 1D $^1$H NMR spectra of (A) $T(CmCTG)_2T$ and (B) $A(CmCTG)_2T$ at pH 7, 6, and 5 in comparison with the reference spectrum of the $(CCTG)_2$ MDB. All spectra were acquired at 0 °C. The H1/H3 and H41/H42 signal intensities were amplified by fourfolds relative to H7 signals.

MDB structure, *e.g.*, an increase in $T_m$ by ∼12 °C was achieved by introducing such hydrophobic interactions.[22] 5-Methylcytosine, which serves as an epigenetic biomarker in gene regulations,[26] has been reported to enhance thermodynamic



https://doi.org/10.1021/acsomega.1c04346
ACS Omega 2021, 6, 28263−28269

Table 2. Thermodynamic Parameters of the $T(CmCTG)_2T$, $A(CmCTG)_2T$, and $TT(CmCTG)_2TT$ MDBs[a]

| MDB | $T_m$ (°C) | $\Delta H°$ (kcal·mol$^{-1}$) | $\Delta S°$ (cal·K$^{-1}$·mol$^{-1}$) | $\Delta G°_{298K}$ (kcal·mol$^{-1}$) |
|---|---|---|---|---|
| $T(CmCTG)_2T$ | 51 ± 2 | −24 ± 1 | −73 ± 3 | −1.9 ± 0.1 |
| $A(CmCTG)_2T$ | 52 ± 2 | −20 ± 1 | −62 ± 4 | −1.66 ± 0.03 |
| $TT(CmCTG)_2TT$ | 45 ± 2 | −12 ± 2 | −38 ± 7 | −0.76 ± 0.08 |

[a]The average and uncertainty values were determined by three replicative UV melting experiments.

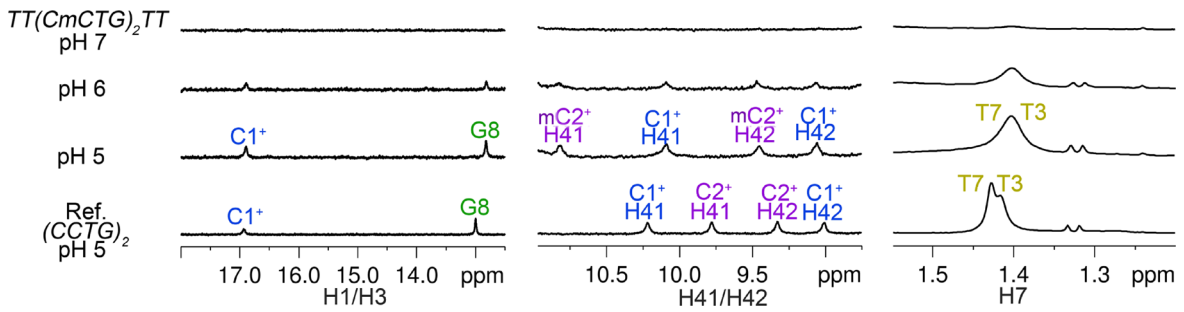


**Figure 4.** 1D $^1$H NMR spectra of $TT(CmCTG)_2TT$ in comparison with the reference spectrum of $(CCTG)_2$ MDB. The spectra were acquired at 0 °C. The intensity scale of the H1/H3 and H41/H42 regions was increased by fourfolds relative to that of the methyl H7 region.

stabilities of various types of DNA structures such as duplexes,[27] triplexes,[28] i-motifs,[29] and G-quadruplexes.[30] Herein, we substituted the minor groove residues (C2 and C6) in $T(CCTG)_2T$ and $A(CCTG)_2T$ with 5-methylcytosine residues and obtained $T(CmCTG)_2T$ and $A(CmCTG)_2T$.

It was found that upon lowering the pH to 5, both $T(CmCTG)_2T$ and $A(CmCTG)_2T$ showed characteristic NMR signals of MDB, including (i) the C1$^+$ H3 at 16.9 ppm and G8 H1 at 12.8 ppm, (ii) downfield shifted C1$^+$ H41/H42 (10.1/9.1 ppm) and mC2$^+$ H41/H42 (10.4/8.9 ppm) signals, and (iii) upfield shifted T3 and T7 H7 signals at 1.4 ppm (Figure 3), all of which agreed with those in the reference $(CCTG)_2$ MDB. These suggested that $T(CmCTG)_2T$ and $A(CmCTG)_2T$ folded into MDB structures bearing 5′ and 3′-overhanging residues at pH 5. Indeed, such characteristic signals were also observed at pH 6 and their peak intensities were similar to those at pH 5, suggesting that C1 and mC2 were almost fully protonated and the MDBs were formed stably at pH 6.

As determined by UV melting experiments, the $T_m$ values of these two MDBs were ∼51 and 52 °C, respectively (Table 2), suggesting that they would predominantly remain folded at room temperature or even physiological temperature. Noticeably, the $T_m$ value of $T(CmCTG)_2T$ or $A(CmCTG)_2T$ was even higher than that of the $(CCTG)_2$ MDB (∼46 °C),[17] revealing the great effectiveness of cytosine methylation in stabilizing the MDB structure.

**2.3. $TT(CmCTG)_2TT$ Formed a Stable MDB Structure.** Upon successful construction of MDBs carrying a 1-nucleotide (nt) overhang at both 5′ and 3′-ends, we wondered if the MDB could sustain longer 5′ and 3′-overhangs. Accordingly, we designed $TT(CmCTG)_2TT$ that carries a 2-nt overhang at both 5′ and 3′-ends. At pH 5, $TT(CmCTG)_2TT$ displayed NMR signatures that are suggestive of the MDB formation (Figure 4), including (i) the C1$^+$ H3 at 16.9 ppm and G8 H1 at 12.8 ppm, (ii) the downfield shifted C1$^+$ H41/H42 (10.1/9.1 ppm) and mC2$^+$ H41/H42 (10.9/9.5 ppm) signals, and (iii) the upfield shifted T3 and T7 H7 signals at 1.4 ppm.

The $T_m$ of the $TT(CmCTG)_2TT$ MDB was determined to be ∼45 °C (Table 2), which was ∼6 °C lower than that of the $T(CmCTG)_2T$ or $A(CmCTG)_2T$ MDB. The $\Delta G°_{298K}$ of $TT(CmCTG)_2TT$ was less negative than that of $T(CmCTG)_2T$ or $A(CmCTG)_2T$ MDB, and this was attributed predominantly to a less favorable $\Delta H°$ and partially compensated by the favorable $\Delta S°$. As suggested by the less negative $\Delta H°$, the longer overhangs in $TT(CmCTG)_2TT$ might lead to a steric hindrance at the terminal junction of the MDB so that the base−base stackings were weakened.

**2.4. Rational Design of a DNA Molecular Switch Based on the $T(CmCTG)_2T$ MDB.** DNA-based molecular switches responding to external stimuli, *e.g.*, pH, metal ion, and light, show potential applications in bio-related research such as biosensing and controlled drug release.[6,19,20] As $T(CmCTG)_2T$, $A(CmCTG)_2T$, and $TT(CmCTG)_2TT$ formed stable MDBs sustaining overhanging residues (Figures 3,4), we wondered if they could be used to construct a DNA molecular switch. To test this, $T(CmCTG)_2T$ was selected for a proof-of-concept study. We first constructed a system that was composed of the $T(CmCTG)_2T$ strand and the *S1-wc* strand. It was anticipated that $T(CmCTG)_2T$ and *S1-wc* could form a duplex containing eight Watson−Crick base pairs in the presence of $Mg^{2+}$ at pH 7 (the "ON" state), while the duplex would dissociate to restore the MDB formation upon inputting EDTA and pH 5 (the "OFF" state), as the MDB would become more stable than the duplex at pH 5 especially when the $Mg^{2+}$ was chelated by EDTA.

CD experiments were performed to monitor the structural conversion. The CD spectrum of $T(CmCTG)_2T$ MDB at pH 5 displayed a positive band at ∼290 nm, which served as a reference spectrum (Figure S1). The CD spectrum of the $T(CmCTG)_2T$ and *S1-wc* mixture in 10 mM NaPi (pH 7) and $Mg^{2+}$ showed a major positive absorption band at ∼265 nm, which was consistent with the CD spectral feature of DNA duplexes[31] and thus suggested the hybridization between $T(CmCTG)_2T$ and *S1-wc* (Figure S1). The CD spectrum of the $T(CmCTG)_2T$ and *S1-wc* mixture in 10 mM NaPi (pH 5), $Mg^{2+}$, and excessive EDTA displayed a positive band at ∼290 nm, which was in line with the CD absorbance of the $T(CmCTG)_2T$ MDB, but unfortunately the positive band at ∼260 nm was still clearly observed (Figure S1). This suggests that the duplex did not fully dissociate upon adjusting the pH to 5 and adding EDTA, probably because the difference in the


https://doi.org/10.1021/acsomega.1c04346
ACS Omega 2021, 6, 28263−28269

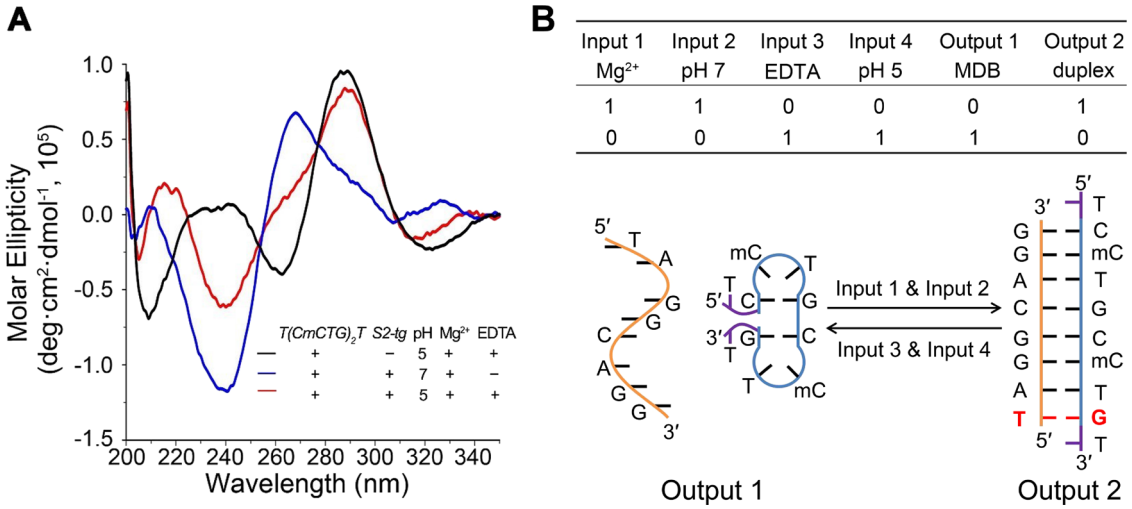


**Figure 5.** (A) CD spectra of the $T(CmCTG)_2T$ MDB in 10 mM NaPi (pH 5), $Mg^{2+}$, and EDTA (black line), the $T(CmCTG)_2T$ and *S2-tg* mixture in 10 mM NaPi (pH 7) and $Mg^{2+}$ (blue line), and the $T(CmCTG)_2T$ and *S2-tg* mixture in 10 mM NaPi (pH 5), $Mg^{2+}$, and EDTA (red line). (B) Truth table (top) and scheme (bottom) of the molecular switch using $T(CmCTG)_2T$ and *S2-tg*.

thermodynamic stability between the $T(CmCTG)_2T$ MDB and the complementary duplex at pH 5 was not large enough.

Based on the above trial, we rationally designed another DNA molecular switch that was composed of $T(CmCTG)_2T$ and *S2-tg*. The duplex, if formed, would contain a T·G mismatch and seven Watson−Crick base pairs. It has been reported that the $T_m$ of the DNA duplex was lowered by 6−7 °C upon substituting one C-G Watson−Crick base pair with a T·G mismatch.[32,33] Therefore, we expected that the thermostability of the duplex formed by $T(CmCTG)_2T$ and *S2-tg* would be lower than that of the duplex formed by $T(CmCTG)_2T$ and *S1-wc*. The CD spectrum of the $T(CmCTG)_2T$ and *S2-tg* mixture in 10 mM NaPi (pH 7) and $Mg^{2+}$ showed a positive band at ∼265 nm (Figure 5A, blue line), suggesting a vast majority of duplex formation. The CD spectrum of the $T(CmCTG)_2T$ and *S2-tg* mixture in 10 mM NaPi (pH 5), $Mg^{2+}$, and excessive EDTA showed a major positive band at ∼290 nm, and the positive band at ∼265 was almost vanished (Figure 5A, red line). This reveals that the usage of a T·G mismatch to lower the thermodynamic stability of the duplex facilitated structural conversion to the MDB at pH 5.

In short, we have successfully constructed an MDB-based molecular switch that is composed of $T(CmCTG)_2T$ and *S2-tg* (Figure 5B). In the presence of pH 7 and $Mg^{2+}$ dual inputs, the system was in an "ON" state, *i.e.*, $T(CmCTG)_2T$ and *S2-tg* formed a duplex. Upon inputting pH 5 and excessive EDTA dual inputs, the system was in an "OFF" state, *i.e.*, $T(CmCTG)_2T$ and *S2-tg* adopted an MDB and a single strand, respectively. The MDB-based molecular switch designed in this study sensitively responds to pH and $Mg^{2+}$/EDTA in a programmable manner, which shows structural conversions at room temperature with an easy manipulation. More importantly, the 5′ and 3′-overhanging residues in the newly designed stable MDBs may be replaced by reporter molecules such as fluorophores to extend the application of MDBs in biosensing.

## 3. CONCLUSIONS

This study, for the first time, demonstrates that the MDB structure could sustain 5′ and 3′-overhanging residues, suggesting the possibility of functionalization of MDBs. The newly designed MDBs remained stable at room temperature or even physiological temperature. A molecular switch based on one of the new MDBs was constructed. Dual inputs of pH 7 and $Mg^{2+}$ could maintain the system in an "ON" state, whereas the dual inputs of pH 5 and EDTA could switch the system to an "OFF" state. The result of this work paves the way for extending the application of an MDB structure in dynamic DNA nanotechnology such as biosensing.

## 4. MATERIALS AND METHODS

**4.1. DNA Sample Preparation.** DNA samples were synthesized using an Applied Biosystems Model 394 DNA/RNA Synthesizer. Phosphoramidites used for DNA synthesis were purchased from ChemGenes Corporation (U.S.A). The synthesized DNA products were purified by denaturing polyacrylamide gel electrophoresis and diethylaminoethyl sephacel anion exchange column chromatography and finally desalted using Amicon Ultra-4 centrifugal filter devices. The UV absorbance at 260 nm was measured for DNA quantitation.

**4.2. NMR Experiments.** NMR samples were prepared by dissolving ∼0.1 μmol purified DNA in 500 μL of 90% $H_2O$/10% $D_2O$ (v/v) solutions containing 0.02 mM 2,2-dimethylsilapentane-5-sulfonic acid (DSS) and 10 mM sodium chloride (NaCl). The pH of NMR samples was adjusted by adding hydrochloric acid (HCl) or sodium hydroxide (NaOH). NMR experiments were conducted on a Bruker AVANCE-500 and/or AVANCE-700 spectrometers. In one-dimensional (1D) $^1$H experiments and two-dimensional (2D) nuclear Overhauser effect spectroscopy (NOESY) experiments, the excitation sculpting pulse sequence[34] was employed to suppress the water signal. The 1D $^1$H spectra were processed by applying an exponential window function with a line broadening of 2 Hz. For 2D NOESY experiments, datasets of 4096 × 512 were acquired and then zero-filled to give 4096 × 4096 spectra with a cosine window function applied to both dimensions. All NMR spectra were acquired at 0 °C unless otherwise specified.

**4.3. $^1$H Resonance Assignments.** Sequential resonance assignments of DNA sequences were made from the NOESY


https://doi.org/10.1021/acsomega.1c04346
ACS Omega 2021, 6, 28263−28269

H6/H8-H1′ fingerprint region using standard methods.[35] The amino proton H41/H42 resonances were assigned based on intra-nucleotide H5-H41/H42 NOEs for cytosine and intra-nucleotide H7-H41/H42 NOEs for 5-methylcytosine. $^1$H resonance assignments of $T(CmCTG)_2T$, $A(CmCTG)_2T$, and $TT(CmCTG)_2TT$ are shown in Figures S2−S7.

**4.4. UV Melting Experiments.** UV melting experiments were carried out to determine the thermodynamic stabilities of $T(CmCTG)_2T$, $A(CmCTG)_2T$, and $TT(CmCTG)_2TT$. Samples for UV melting experiments were prepared to contain 5 $\mu$M DNA in 1000 $\mu$L buffer solutions containing 10 mM sodium phosphate (NaPi) at pH 5. A cuvette with a path length of 10 mm was used. The absorbance at 260 nm was monitored as a function of temperature using a Hewlett−Packard 8453 diode-array UV−visible spectrophotometer, and the temperature was measured by a BetaTHERM thermistor temperature sensor inserted into the cuvette. The absorbance was measured from 25 to 80 °C for $T(CmCTG)_2T$, from 20 to 80 °C for $A(CmCTG)_2T$, and from 15 to 80 °C for $TT(CmCTG)_2TT$, with a step size of 1 °C and a holding time of 1 min. Thermodynamic parameters, including the $T_m$, change in enthalpy ($\Delta H°$), change in entropy ($\Delta S°$), and change in Gibbs free energy ($\Delta G°_{298K}$), were obtained by fitting the melting profiles with a two-state transition model.[36] Three replicative UV melting measurements were conducted for each DNA sequence.

**4.5. Circular Dichroism (CD) Experiments.** To monitor the molecular switching process in our designed DNA molecular switch, CD experiments were performed using a Chirascan V100 CD spectrometer with a bandwidth of 1 nm at room temperature. Five CD samples were prepared, including (i) 15 $\mu$M $T(CmCTG)_2T$ in 10 mM NaPi (pH 5), $MgCl_2$, and EDTA, (ii) 15 $\mu$M $T(CmCTG)_2T$ and *S1-wc* in 10 mM NaPi (pH 7) and $MgCl_2$, (iii) 15 $\mu$M $T(CmCTG)_2T$ and *S1-wc* in 10 mM NaPi (pH 5), $MgCl_2$, and EDTA, (iv) 15 $\mu$M $T(CmCTG)_2T$ and *S2-tg* in 10 mM NaPi (pH 7) and $MgCl_2$, and (v) 15 $\mu$M $T(CmCTG)_2T$ and *S2-tg* in 10 mM NaPi (pH 5), $MgCl_2$, and EDTA. The CD sample was placed in a cuvette of 0.5 mm path length, and the CD spectrum was collected from 200 to 350 nm with a step size of 1 nm. For each sample, three replicates of scans were acquired, and an average value was taken. The CD spectra were background corrected using the corresponding buffer solution.

## ■ ASSOCIATED CONTENT

### Supporting Information

The Supporting Information is available free of charge at https://pubs.acs.org/doi/10.1021/acsomega.1c04346.

$^1$H NMR assignments of $T(CmCTG)_2T$, $A(CmCTG)_2T$, and $TT(CmCTG)_2TT$, and additional CD spectra (PDF)

## ■ AUTHOR INFORMATION


### Corresponding Authors

**Yuan Liu** − *South China Advanced Institute for Soft Matter Science and Technology, School of Molecular Science and Engineering, South China University of Technology, Guangzhou, Guangdong 510640, China*; Email: derekliu@scut.edu.cn

**Pei Guo** − *School of Biology and Biological Engineering, South China University of Technology, Guangzhou, Guangdong 510006, China*; orcid.org/0000-0001-7760-5786; Email: peiguo@scut.edu.cn

### Authors

**Jiacheng Zhang** − *School of Biology and Biological Engineering, South China University of Technology, Guangzhou, Guangdong 510006, China*

**Yang Wang** − *School of Biology and Biological Engineering, South China University of Technology, Guangzhou, Guangdong 510006, China*

**Liqi Wan** − *Department of Chemistry, The Chinese University of Hong Kong, Hong Kong, China*; orcid.org/0000-0003-3663-2678

**Jie Yi** − *School of Biology and Biological Engineering, South China University of Technology, Guangzhou, Guangdong 510006, China*

**Sik Lok Lam** − *Department of Chemistry, The Chinese University of Hong Kong, Hong Kong, China*; orcid.org/0000-0001-5368-706X

Complete contact information is available at: https://pubs.acs.org/10.1021/acsomega.1c04346

### Author Contributions

#J.Z. and Y.W. contributed equally to this work.


### Notes

The authors declare no competing financial interest.

## ■ ACKNOWLEDGMENTS

This work was supported by the National Natural Science Foundation of China (Project ID: 22004038), the Natural Science Foundation of Guangdong Province, China (Project ID: 2021A1515010102), and the Basic and Applied Basic Research Foundation of Guangzhou, Guangdong, China (Project ID: 202102020066).

## ■ REFERENCES


(1) Hu, Y.; Cecconello, A.; Idili, A.; Ricci, F.; Willner, I. Triplex DNA Nanostructures: From Basic Properties to Applications. *Angew. Chem. Int. Ed. Engl.* **2017**, *56*, 15210−15233.

(2) Zheng, J.; Du, Y.; Wang, H.; Peng, P.; Shi, L.; Li, T. Ultrastable Bimolecular G-Quadruplexes Programmed DNA Nanoassemblies for Reconfigurable Biomimetic DNAzymes. *ACS Nano* **2019**, *13*, 11947−11954.

(3) Dong, Y.; Yang, Z.; Liu, D. DNA Nanotechnology Based on I-motif Structures. *Acc. Chem. Res.* **2014**, *47*, 1853−1860.

(4) Satange, R.; Chang, C. K.; Hou, M. H. A Survey of Recent Unusual High-resolution DNA Structures Provoked by Mismatches, Repeats and Ligand Binding. *Nucleic Acids Res.* **2018**, *46*, 6416−6434.

(5) Abdelhamid, M. A.; Fabian, L.; MacDonald, C. J.; Cheesman, M. R.; Gates, A. J.; Waller, Z. A. Redox-Dependent Control of I-Motif DNA Structure Using Copper Cations. *Nucleic Acids Res.* **2018**, *46*, 5886−5893.

(6) Mergny, J. L.; Sen, D. DNA Quadruple Helices in Nanotechnology. *Chem. Rev.* **2019**, *119*, 6290−6325.

(7) Asamitsu, S.; Bando, T.; Sugiyama, H. Ligand Design to Acquire Specificity to Intended G-Quadruplex Structures. *Chem. − Eur. J.* **2019**, *25*, 417−430.

(8) Liu, N.; Liedl, T. DNA-Assembled Advanced Plasmonic Architectures. *Chem. Rev.* **2018**, *118*, 3032−3053.

(9) Choi, J. H.; Lim, J.; Shin, M.; Paek, S. H.; Choi, J. W. CRISPR-Cas12a-Based Nucleic Acid Amplification-Free DNA Biosensor via Au Nanoparticle-Assisted Metal-Enhanced Fluorescence and Colorimetric Analysis. *Nano Lett.* **2021**, *21*, 693−699.

(10) Chen, X.; Chen, T.; Ren, L.; Chen, G.; Gao, X.; Li, G.; Zhu, X. Triplex DNA Nanoswitch for pH-Sensitive Release of Multiple Cancer Drugs. *ACS Nano* **2019**, *13*, 7333−7344.
(11) Hu, Q.; Li, H.; Wang, L.; Gu, H.; Fan, C. DNA Nanotechnology-Enabled Drug Delivery Systems. *Chem. Rev.* **2019**, *119*, 6459−6506.
(12) Hu, Z.; Suo, Z.; Liu, W.; Zhao, B.; Xing, F.; Zhang, Y.; Feng, L. DNA Conformational Polymorphism for Biosensing Applications. *Biosens. Bioelectron.* **2019**, *131*, 237−249.
(13) Shi, L.; Cao, F.; Zhang, L.; Tian, Y. I-motif Formed at Physiological pH Triggered by Spatial Confinement of Nanochannels: an Electrochemical Platform for pH Monitoring in Brain Microdialysates. *Anal. Chem.* **2020**, *92*, 4535−4540.
(14) Guo, P.; Lam, S. L. Minidumbbell: a New Form of Native DNA Structure. *J. Am. Chem. Soc.* **2016**, *138*, 12534−12540.
(15) Guo, P.; Lam, S. L. Minidumbbell Structures Formed by ATTCT Pentanucleotide Repeats in Spinocerebellar Ataxia Type 10. *Nucleic Acids Res.* **2020**, *48*, 7557−7568.
(16) Guo, P.; Lam, S. L. The Competing Mini-dumbbell Mechanism: New Insights into CCTG Repeat Expansion. *Signal Transduction Targeted Ther.* **2016**, *1*, 16028.
(17) Guo, P.; Lam, S. L. An Extraordinarily Stable DNA Minidumbbell. *J. Phys. Chem. Lett.* **2017**, *8*, 3478−3481.
(18) Wan, L.; Lam, S. L.; Lee, H. K.; Guo, P. Rational Design of a Reversible $Mg^{2+}$/EDTA-Controlled Molecular Switch Based on a DNA Minidumbbell. *Chem. Commun.* **2020**, *56*, 10127−10130.
(19) Qi, H.; Yue, S.; Bi, S.; Ding, C.; Song, W. DNA Logic Assembly Powered by a Triplex-Helix Molecular Switch for Extracellular pH Imaging. *Chem. Commun.* **2018**, *54*, 8498−8501.
(20) Simmel, F. C.; Yurke, B.; Singh, H. R. Principles and Applications of Nucleic Acid Strand Displacement Reactions. *Chem. Rev.* **2019**, *119*, 6326−6369.
(21) Ngai, C. K.; Lam, S. L.; Lee, H. K.; Guo, P. High-Resolution Structures of DNA Minidumbbells Comprising Type II Tetraloops with a Purine Minor Groove Residue. *J. Phys. Chem. B* **2020**, *124*, 5131−5138.
(22) Guo, P.; Lam, S. L. Unprecedented Hydrophobic Stabilizations from a Reverse Wobble T·T Mispair in DNA Minidumbbell. *J. Biomol. Struct. Dyn.* **2020**, *38*, 1946−1953.
(23) Isaksson, J.; Chattopadhyaya, J. A Uniform Mechanism Correlating Dangling-End Stabilization and Stacking Geometry. *Biochemistry* **2005**, *44*, 5390−5401.
(24) Ambrus, A.; Chen, D.; Dai, J.; Jones, R. A.; Yang, D. Solution Structure of the Biologically Relevant G-Quadruplex Element in the Human c-MYC Promoter. Implications for G-Quadruplex Stabilization. *Biochemistry* **2005**, *44*, 2048−2058.
(25) Do, N. Q.; Phan, A. T. Monomer-Dimer Equilibrium for the 5′-5′ Stacking of Propeller-Type Parallel-Stranded G-Quadruplexes: NMR Structural Study. *Chem. − Eur. J.* **2012**, *18*, 14752−14759.
(26) Greenberg, M. V. C.; Bourc'his, D. The Diverse Roles of DNA Methylation in Mammalian Development and Disease. *Nat. Rev. Mol. Cell Biol.* **2019**, *20*, 590−607.
(27) Thalhammer, A.; Hansen, A. S.; El-Sagheer, A. H.; Brown, T.; Schofield, C. J. Hydroxylation of Methylated CpG Dinucleotides Reverses Stabilisation of DNA Duplexes by Cytosine 5-Methylation. *Chem. Commun.* **2011**, *47*, 5325−5327.
(28) Leitner, D.; Schröder, W.; Weisz, K. Influence of Sequence-Dependent Cytosine Protonation and Methylation on DNA Triplex Stability. *Biochemistry* **2000**, *39*, 5886−5892.
(29) Wright, E. P.; Abdelhamid, M. A. S.; Ehiabor, M. O.; Grigg, M. C.; Irving, K.; Smith, N. M.; Waller, Z. A. E. Epigenetic Modification of Cytosines Fine Tunes the Stability of I-motif DNA. *Nucleic Acids Res.* **2020**, *48*, 55−62.
(30) Lin, J.; Hou, J. Q.; Xiang, H. D.; Yan, Y. Y.; Gu, Y. C.; Tan, J. H.; Li, D.; Gu, L. Q.; Ou, T. M.; Huang, Z. S. Stabilization of G-Quadruplex DNA by C-5-Methyl-Cytosine in Bcl-2 Promoter: Implications for Epigenetic Regulation. *Biochem. Biophys. Res. Commun.* **2013**, *433*, 368−373.
(31) Kypr, J.; Kejnovska, I.; Renciuk, D.; Vorlickova, M. Circular Dichroism and Conformational Polymorphism of DNA. *Nucleic Acids Res.* **2009**, *37*, 1713−1725.
(32) Owczarzy, R.; You, Y.; Groth, C. L.; Tataurov, A. V. Stability and Mismatch Discrimination of Locked Nucleic Acid-DNA Duplexes. *Biochemistry* **2011**, *50*, 9352−9367.
(33) Oliveira, L. M.; Long, A. S.; Brown, T.; Fox, K. R.; Weber, G. Melting Temperature Measurement and Mesoscopic Evaluation of Single, Double and Triple DNA Mismatches. *Chem. Sci.* **2020**, *11*, 8273−8287.
(34) Stott, K.; Stonehouse, J.; Keeler, J.; Hwang, T.-L.; Shaka, A. J. Excitation Sculpting in High-Resolution Nuclear Magnetic Resonance Spectroscopy: Application to Selective NOE Experiments. *J. Am. Chem. Soc.* **1995**, *117*, 4199−4200.
(35) Wijmenga, S. S.; van Buuren, B. N. M. The Use of NMR Methods for Conformational Studies of Nucleic Acids. *Prog. Nucl. Magn. Reson. Spectrosc.* **1998**, *32*, 287−387.
(36) Greenfield, N. J. Using Circular Dichroism Collected as a Function of Temperature to Determine the Thermodynamics of Protein Unfolding and Binding Interactions. *Nat. Protoc.* **2006**, *1*, 2527−2535.


https://doi.org/10.1021/acsomega.1c04346
*ACS Omega* 2021, 6, 28263−28269